Malaysian Journal of Chemistry, 2013, Vol. 15, No. 1, 067 – 076

Thermodynamic and Interfacial Studies of Co-crystals of 8-Hydroxyquioniline – Urea System

H. Shekhar, Jaisheel Kumar[1] and C. S. Saha[2]
Department of Chemistry, V. K. S. University, Ara, 802301
[1]Department of Physics, V. K. S. University, Ara, 802301
[2]Principal, M. V. College, Buxar,
e-mail – hshe2503@rediffmail.com
jaisheelng@gmail.com

Abstract : Co-crystals of 8-Hydroxyquinoline (HQ) with Urea (U) has been prepared through melting method. The phase diagram in terms of temperature-composition curve shows the formation of additive co-crystal/ molecular complex (C) between HQ and U and also indicates that the stoichiometry of addition compound is 1:2 followed by two side by side eutectics (E1 and E2). Thermodynamic excess quantities of the system highlight the molecular interaction, structure, stability and ordering of components in the binary melts. The negative value of Gibb's mixing quantity (ΔG^M) for all the eutectic and non-eutectic co-crystals suggests that there is spontaneous mixing in all the cases. The partial molar enthalpy of mixing (ΔH_{HQ}^{-M}) – composition plot shows a maxima on the curve of the binary system which infers that there is a stable interaction between the components at that stoichiometry. The interfacial energy (σ), Gibbs – Thomson coefficient (τ), grain boundary energy (σ_{gb}), critical size or nucleus (r*), driving force of solidification (ΔG_v) and roughness parameter (α) have also been determined using the heat of fusion data of the component. The calculated critical size of the nucleus was found to be in nano-scale. The value for r* for HQ and U lie between 48 ± 1 nm to 170 ± 1 nm and 32 ± nm to 113 ± 1 nm respectively at undercooling 1°C – 3.5°C. This report may explore a bright future for the growth of desired materials with potential application.

Keywords: Phase diagram, heat of fusion, thermodynamic excess and mixing functions, interfacial energy, critical size of nucleus, roughness parameter.

Received : 25.01.2013; Accepted : 23.09.2013

Introduction

The past decades have witnessed a significant increase in research in the field of organic solid-state materials[1-3] for their applications in molecular electronics, optical applications, pharmaceuticals, supramolecules and crystal engineering approaches. The designing of novel molecular solids should be achieved through the construction of multi component molecular solids or co-crystals. The charge transfer organic solids[4,5] are presently being used as photovoltaic, light emitting materials, semiconductors, organic metals and superconductors. These materials have been described as excellent electronic, magnetic and optical properties which may have the capacity to change the faces of the molecular electronic devices. For organic materials exhibiting emission of white and full colour lights in high intensity, many researchers have been extended to get different hole transporting (HT) and electron-transporting (ET) materials for different optoelectronic devices. Since Tang and Van Slyke[6] initially employed vacuum deposition in 1987 for the formation of double organic light-emitting diodes (OLED) with diamine as the hole-transport (HT) materials and 8-hydroxyquinoline aluminium[7] (Alq_3) as the emitting and electron-transporting (ET) material, small organic and polymer light emitting materials have attracted extensive interest in this field. 8-Hydroxyquinoline is a bi-functional hydrogen-bonding molecule, which in aqueous or alcohol solution simultaneously acts as an H-donor at the OH site and an acceptor at the N-atom. Upon photo-excitation, the acid/base properties of this molecule change significantly at the sites, rending OH- group more acidic and the N-atom more basic. HQ and its derivatives are capable of forming complexes with many metal ions[8,9]. In recent years, metal chelates of HQ have played an important role in organic electroluminescence (OLE), and were widely introduced in OLE cell as emission layer[10]. Some HQ derivatives are expected to exhibit non-linear optical (NLO) properties[11]. The quenching of green fluorescence of 8-quinolinolium cations in solutions of low acidity has been attributed to the prototropic equilibrium in the S_1 state between 8-quinolinolium cations and the non-fluorescence zwitterions[12] form of HQ. The fluorescence of

HQ was studied in several media and concluded that quenching of fluorescence is due to H-bonding by the hydroxylic solvents[13]. Urea is one of the prototypical molecules used in the study of nonlinear optical (NLO) properties of molecular systems[14]. With view to search and achieve a new and better performing OLED, 8-Hydroxyquinoline (HQ) with Urea (U) has been selected as binary system for their detailed investigations such as the phase diagram, molecular interaction, thermodynamic excess and mixing functions, thermal stability, driving force of nucleation during solidification (ΔG_v), critical size or radius (r*) and the critical free energy of nucleation (ΔG^*) at different undercoolings of binary materials have been determined. Using heat of fusion data the solid-liquid interface energy (σ), grain boundary energy (σ_{gb}), the Gibbs-Thomson coefficient (τ) and roughness parameter (α) of all the alloys are evaluated by numerical method. Interface morphology of the alloys follows the Jackson's surface roughness (α) theory and predicts the faceted growth proceeds in all the alloys optical materials.

Experimental Procedure

8-Hydroxyquinoline (HQ) (Thomas Baker, Mumbai) and Urea (U) (Thomas Baker, Mumbai) were used directly without further purification. The melting point of 8-Hydroxyquinoline (HQ) was determined to be 74°C while Urea (U) was melted at 133°C. For measuring the solid-liquid equilibrium data of HQ-U system, mixtures of different composition were made in glass test tubes by repeated heating and followed by chilling in ice and was determined by the thaw-melt method[15]. The melting and thaw temperatures were determined in a Toshniwal melting point apparatus using a precision thermometer which could read accurately to ± 0.1°C. The heater was regulated to give above 1°C increase in temperature in every five minutes. Heat of fusion of materials was measured by the DTA method[16] using NETZSCH Simultaneous Thermal Analyzer, STA 409 series unit.

Results and discussion

Phase diagram

The solid liquid equilibrium data for HQ-U system is reported in the form of temperature/composition curve (Fig 1) which indicates that the system exhibits the formation 1:2 additive co-crystals/ molecular complex C surrounded by two eutectic co-crystals E1 and E2. The melting temperature of C (120^0C), E1(71^0C) and E2(80^0C) and their compositions are at 0.665, 0.530 and 0.745 mole fraction of Urea. On addition of U in HQ the melting point of the mixture decreases and attains the minimum at E1 (the first eutectic of the system). On continued addition of HQ the melting point rises and attains the maximum at 'C' where the, composition of solid and liquid phase are identical. This is the congruent melting point of the compound formed in the system. A further increase in concentration of U cause a decrease in the melting point till the minimum E2 (the second eutectic of the system) is attained. A good length of the middle branch of the curve and the existence of a eutectic point on both side of the maximum leads the information regarding the stability of C. This co-crystal C is formed by the reaction between the two components in the following manner

A (solid) + B (solid) $\rightleftharpoons$ **AB (liquid)**

$\rightleftharpoons$ **AB (solid)**

For each eutectic co-crystals (E1 and E2) the additive co-crystal C serves as one of the components. The existence of co-crystals A1 to A11 has been shown in the diagram in binary solid form. The observed maxima in the system under investigation found flat, indicates that the addition compound is dissociated in molten state. From phase diagram it can be inferred that the addition compounds in this system is capable of existing in solid form in equilibrium with a liquid of the same composition.

Thermodynamic Studies

The values of heats of fusion of 1:2 co-crystal C, eutectic and noneutectic co-crystals are calculated by the mixture law. The value of heat of fusion of co-crystals A1-A11, E1and E2 is reported in Table 1. The activity coefficient and activity of components for the systems under investigation has been calculated from the equation[17] given below

$$-\ln x_i \gamma_i = \frac{\Delta H_i}{R}\left(\frac{1}{T_e} - \frac{1}{T_i}\right) \qquad (1)$$

where γ_i is activity coefficient of the component *i* in the liquid phase respectively, ΔH_i is the heat of fusion of component i at melting point T_i and R is the gas constant. T_e is the melting temperature of alloy. Using the values of activity and activity coefficient of the components in alloys mixing and excess thermodynamics functions have been computed.

Mixing Functions

The mixing behaviour of components in the alloy is decided by the value of Gibbs' free energy of mixing in the system. For illustrating it integral molar free energy of mixing (ΔG^M),

molar entropy of mixing (ΔS^M) and molar enthalpy of mixing (ΔH^M) and partial thermodynamic mixing functions of the binary alloys were determined by using the following equations

$$\Delta G^M = RT\,(\chi_{HQ} \ln a_{HQ} + \chi_U \ln a_U) \quad (2)$$

$$\Delta S^M = -R\,(\chi_{HQ} \ln\chi_{HQ} + \chi_U \ln\chi_U) \quad (3)$$

$$\Delta H^M = RT\,(\chi_{HQ} \ln\gamma_{HQ} + \chi_U \ln\gamma_U) \quad (4)$$

$$G^{-}_i{}^M = \mu^{-}_i{}^M = RT \ln a_i \quad (5)$$

where $G^{-}_i{}^M$ ($\mu^{-}_i{}^M$) is the partial molar free energy of mixing of component i (mixing chemical potential) in binary mix. and γ_i and a_i is the activity coefficient and activity of component respectively. The negative value[18] of molar free energy of mixing of alloys (Table 2) suggests that the mixing in all cases is spontaneous. The integral molar enthalpy of mixing value corresponds to the value of excess integral molar free energy of the system favouring regular solutions theory.

Excess Functions

With a view to describe the nature of the interactions between the components forming the eutectic and non-eutectic co-crystals, the excess thermodynamic functions such as integral excess integral free energy (g^E), excess integral entropy (s^E) and excess integral enthalpy (h^E) were calculated using the following equations (6), (7) and (8) , and excess chemical potential or excess partial free energy of mixing (9).

$$g^E = RT(\chi_{HQ} \ln \gamma_{HQ} + x_U \ln \gamma_U) \quad (6)$$

$$s^E = -R\left((\chi_{HQ} \ln \gamma_{HQ} + \chi_U \ln \gamma_U + \chi_{HQ} T \frac{\delta \ln \gamma_{HQ}}{\delta T} + \chi_U T \frac{\delta \ln \gamma_U}{\delta T} \right) \quad (7)$$

$$h^E = -RT^2\left(\chi_{HQ} \frac{\delta \ln \gamma_{HQ}}{\delta T} + \chi_U \frac{\delta \ln \gamma_U}{\delta T} \right) \quad (8)$$

$$g_i^{-E} = \mu_i^{-M} = RT \ln \gamma_i \quad (9)$$

The values of $\delta \ln\gamma_i / \delta T$ can be determined by the slope of liquidus curve near the alloys form in the phase diagram. The values of the excess thermodynamic functions are given in Table 3. The value of the excess free energy is a measure of the departure of the system from ideal behavior. The reported excess thermodynamic data substantiate the earlier conclusion of an appreciable interaction between the parent components during the formation of alloys. The positive g^E value[19] for all eutectic and non-eutectic co-crystals infers stronger interaction between like molecules in binary mix. The excess entropy is a measure of the change in configurational energy due to a change in potential energy and indicates an increase in randomness.

Gibbs-Duhem Equation

Further, the partial molar quantity, activity and activity coefficient can also be determined by using Gibbs-Duhem equation[20]

$$\sum x_i dz_i^{-M} = 0 \quad (10)$$

$$or\ \ \chi_{HQ} dH_{HQ}^{-M} + \chi_U dH_U^{-M} = 0 \quad (11)$$

$$or \quad dH_{HQ}^{-M} = \frac{\chi_U}{\chi_{HQ}} dH_U^{-M} \tag{12}$$

$$or \quad [H_{HQ}^{-M}]_{\chi_{HQ}=y} = \int_{\chi_{HQ}=y}^{\chi_{HQ}=1} \frac{\chi_U}{\chi_{HQ}} dH_U^{-M} \tag{13}$$

Using equation (13) a graph between H_U^{-M} and χ_U/χ_{HQ} gives the solution of the partial molar heat of mixing of component HQ in HQ/U alloy and plot between χ_U/χ_{HQ} vs $\ln a_U$ determines the value of activity of component HQ in binary alloys.

Interfacial Studies

The Effective Entropy Change (ΔS_v)

It is obvious that the effective entropy change and the volume fraction of phases in the alloy are inter-related to decide the interface morphology during solidification and the volume fraction of the two phases depends on the ratio of effective entropy change of the phases. The entropy of fusion ($\Delta S = \Delta H/T$) value (Table 1) of alloys is calculated by heat of fusion values of the materials. The effective entropy change per unit volume (ΔS_V) is given by

$$\Delta S_V = \frac{\Delta H}{T} . \frac{1}{V_m} \tag{14}$$

where ΔH is the enthalpy change, T is the melting temperature and V_m is the molar volume of solid phase. The entropy of fusion per unit volume (ΔS_V) for HQ and U was found 317 and 754 $kJK^{-1}m^{-3}$ respectively. Values of ΔS_V for alloys are reported in Table 1.

The Solid-Liquid Interfacial Energy (σ)

The experimental observation for measuring the value of interfacial energy 'σ' consists a variation in its results about 50-100% from one worker to other. However, Singh and Glickman[21] theoretically calculated the solid-liquid interfacial energy (σ) from melting enthalpy change and obtained the values were in good agreement with the experimental values. Turnbull empirical relationship[22] between molar volume and enthalpy change provides the clue to determine the interfacial energy value of co-crystals and is expressed as:

$$\sigma = \frac{C\Delta H}{(N)^{1/3}(V_m)^{2/3}} \tag{15}$$

where the coefficient *C* lies between 0.33 to 0.35 for nonmetallic system, V_m is molar volume and N is the Avogadro's constant. The value of the solid-liquid interfacial energy of 8-Hydroxyquinoline and Urea was found to be 2.705×10^{-02} and 4.268×10^{-02} J m^{-2} respectively and σ value of alloys was given in Table 1.

Gibbs-Thomson Coefficient (τ)

The Gibbs-Thomson coefficient (τ) of a planar grain boundary acting on planar solid-liquid interface in the system can be calculated by the Gibbs-Thomson equation is expressed as

$$\tau = r\Delta T = \frac{TV_m\sigma}{\Delta H} = \frac{\sigma}{\Delta S_V} \tag{16}$$

where τ is the Gibbs-Thomson coefficient, ΔT is the dispersion in equilibrium temperature and, r is the radius of grooves of interface. The theoretical basis for determination of τ was made for equal thermal conductivities of solid and liquid phases for some transparent materials. It was also determined by the help of Gunduz and Hunt numerical method[23] for materials having known grain boundary shape, temperature gradient in solid and the ratio of thermal conductivity of the equilibrated liquid phases to solid phase ($R = K_L/K_S$).The Gibbs-Thomson coefficient for HQ, U and their alloys are found in the range of 1.65 – 1.09 x 10^{-05} Km and is reported in Table 1.

Interfacial Grain Boundary Energy (σ_{gb})

Grain boundary is the internal surface which can be understood in a very similar way to nucleation on surfaces in liquid-solid transformation. In past, a numerical method is applied to observe the interfacial grain boundary energy (σ_{gb}) without applying the temperature gradient for the grain boundary groove shape. For isotropic interface there is no difference in the value of interfacial tension and interfacial energy. A considerable force is employed at the grain boundary groove in anisotropic interface. The grain boundary energy can be obtained by the equation:

$$\sigma_{gb} = 2\sigma\cos\theta \tag{17}$$

where θ is equilibrium contact angle precipitates at solid-liquid interface of grain boundary. The grain boundary energy could be twice the solid-liquid interfacial energy in the case where the contact angle tends to zero. The value of σ_{gb} for solid HQ and U was found to be 5.226 x 10^{-2} and 8.245 x 10^{-2}Jm^{-2} respectively and the value for all alloys is given in Table 1.

The Critical Radius (r*)

In fact nuclei are rapidly dispersed in unsaturated liquid during liquid-solid transformation and on undercooling liquid becomes saturated and provide nuclei of a critical size with radius r* for nucleation which can be expressed in the light of Chadwick relation[24]

$$r^* = \frac{2\sigma}{\Delta G_V} = \frac{2\sigma T}{\Delta H_V \Delta T} \qquad (18)$$

where σ is the interfacial energy and ΔH_V is the enthalpy of fusion of the compound per unit volume, respectively. The critical size of the nucleus for the components and alloys was calculated at different undercoolings and values are presented in Table 5. It can be inferred from table that the size of the critical nucleus decreases with increase in the undercooling of the melt. The existence of nuclei and a range of nuclei size can be expected in the liquid at any temperature.

The Driving Force of Nucleation (ΔG_v)

During growth of crystalline solid there is change in enthalpy, entropy and specific volume and non-equilibrium leads Gibb's energy. Thermodynamically metastable phase occurs in a supersaturated or super-cooled liquid. The driving force for liquid-solid transition is the difference in Gibb's energy between the two phases. The theories of solidification process in past have been discussed on the basis of diffusion model, kinetic characteristics of nucleation and on thermodynamic features. The lateral motion of rudementry steps in liquid advances stepwise/ non-uniform surface at low driving force while continuous and uniform surface advances at sufficiently high driving force. The driving force of nucleation from liquid to solid during solidification (ΔG_V) can be determined at different undercoolings (ΔT) by using the following equation[25]

$$\Delta G_V = \Delta S_v \Delta T \qquad (19)$$

It is opposed by the increase in surface free energy due to creation of a new solid-liquid interface. By assuming that solid phase nucleates as small spherical cluster of radius arising due to random motion of atoms within liquid. The value of ΔG_V for alloys and pure components are shown in the Table 4.

Critical Free Energy of Nucleation (ΔG^*)

For existence of critical nucleus, it is required to have a localized critical free energy of nucleation (ΔG*) which is evaluated[26] as

$$\Delta G^* = \frac{16}{3}\frac{\pi\sigma^3}{\Delta G_v^2} \qquad (20)$$

The value of ΔG* for alloys and pure components has been found in the range of 10^{-15} to 10^{-16} J at different undercoolings, and has been reported in Table 6.

Interface Morphology

The science of growth has been developed on the foundation of thermodynamics, kinetics, fluid dynamics, crystal structures and interfacial sciences. The solid-liquid interface morphology can be predicted from the value of the entropy of fusion. According to Hunt and Jackson[27], the type of growth from a binary melt depends upon a factor α, defined as:

$$\alpha = \xi\frac{\Delta H}{RT} = \xi\frac{\Delta S}{R} \qquad (21)$$

where ξ is a crystallographic factor depending upon the geometry of the molecules and has a value less than or equal to one. ΔS/R (also known as Jackson's roughness parameter α) is the entropy of fusion (dimensionless) and R is the gas constant. When α is less than two the solid-liquid interface is atomically rough and exhibits non-faceted growth. The value of Jackson's roughness parameter (ΔS/R) is given in Table 1. For the entire co-crystals the α value was found greater than 2 which indicate the faceted growth[28] proceeds in all the cases.

Acknowledgement

Thanks are due to the Head Department of Chemistry, V K S University Ara 802301, India for providing research facilities.

References

1. Arumanayagam, T., and Murugakoothan, P. (2011) *Journal of Minerals & Materials Characterization & Engineering*, **10** (13), 1225-1231.
2. Soroka, K, Vithanage, R. S., Phillips, D. A., Walkar, B. and Dasgupta, P. K. (1987) *Anal. Chem.*, **59**, 629.
3. Zhang, L. G., Ren, X. G., Jiang, D. P., Lu, A. D. and Yuan, J. S. (1996) *Spectros Lett*., **29**, 995.
4. Bader, M. M., Hamada, T., and Kakuta, A. (1992) *J Am. Chem. Soc*., **114**, 6475.

5. Goldman, M., and Wehry, E. L. (1970) Annual Chem., **42**, 1178.
6. Tang, C. W., Van Slyke, S. A., Chen, C.H. J. (1989) *Appl. Phys. Lett*., **65**, 3610.
7. Silva, V. M. and Pereira, L. (2006) *J. Non-Crystalline Solids*, **352**, 5429-5436.
8. Thejo Kalyani, N., Dhoble, S. J., Pode, R. B. (2011) *Adv. Mat. Lett.*, **2 (1)**, 65-70.
9. Abhishek P., Kulkarni, Christopher J. Tonzola, Amit Babel, and Samson A. Jenekhe (2004*) Chem. Mater.*, **16**, 4556-4573.
10. Lim, M. Y., Yunus, W. M. M., Talib, Z. A., Kassim, A., Dee, C. F. and Ismail, A. (2010) *Am. J. of Engineering and Applied Sciences*, **3 (1)**, 64-67.
11. Kido, Kohda, J. (2002) *M. Chem. Rev*., **102**, 2357.
12. Adachi, C., Tokito, S., Tsutsui T., Saito, S. (1988) *Jpn. J. Appl. Phys*., **27**, 269.
13. Heil, H., Steiger, J., Schmechel, R., Von Seggerm (2001) *H. J. Appl. Phys.*, **90**, 10.
14. David A. Dixon (1994) *J. Phy. Chem*., **98**, 3967-3977.
15. Sharma, B. L. (2003) Materials Chemistry and Physics, **78** (3), 691-701.
16. Shekhar, H., Pandey, K. B., and Vishnu Kant (2010) *J. Nat. Acd. Sci. Letter*, **33**, 153-160.
17. Rai, R. N. and Varma, K. B. R. (2001) *Materials Letters*, **48** (6), 356-361.
18. Shekhar, H. and Salim, S. S. (2011) *J. Nat. Acad. Sci Letter*, **34**, 117-125.
19. James W. Rice and Eric M. Suuberg (2010) *J Chem Thermodyn.*, November **42** (11), 1356–1360.
20. Shekhar, H. and Vishnu Kant (2012) International Research Journal of Pharmacy, **3 (5)**, 228-233.
21. Singh, N. B., Glicksman, M. E. (1989) *J. Cryst. Growth*, **98**, 573-580.
22. Turnbull, D. (1950) J. Chem. Phys., **18**, 768.
23. Gunduz, M. and Hunt, J. D. (1989) Acta Metall., **37**, 1839.
24. Chadwick, G. A. (1972) "Mettalography of Phase Transformation," Butterworths, London,.
25. Shekhar, H. and Vishnu Kant (2012) *Asian Journal of Chemistry*, **24** (12),
26. Hillig, W. B. and Turnbull, D. (1956) *Journal of Chemical Physics*, **24 (4)**, 914.
27. Hunt, J. D., Jackson, K. A. (1966) Trans. Metall. Soc. AIME, **236**, 843.
28. Singh, N. B, Tanvi Agrawal, Preeti Gupta and Shiva Saran Das (2009) *J. Chem. Eng. Data*, **54** (5), 1529–1536.

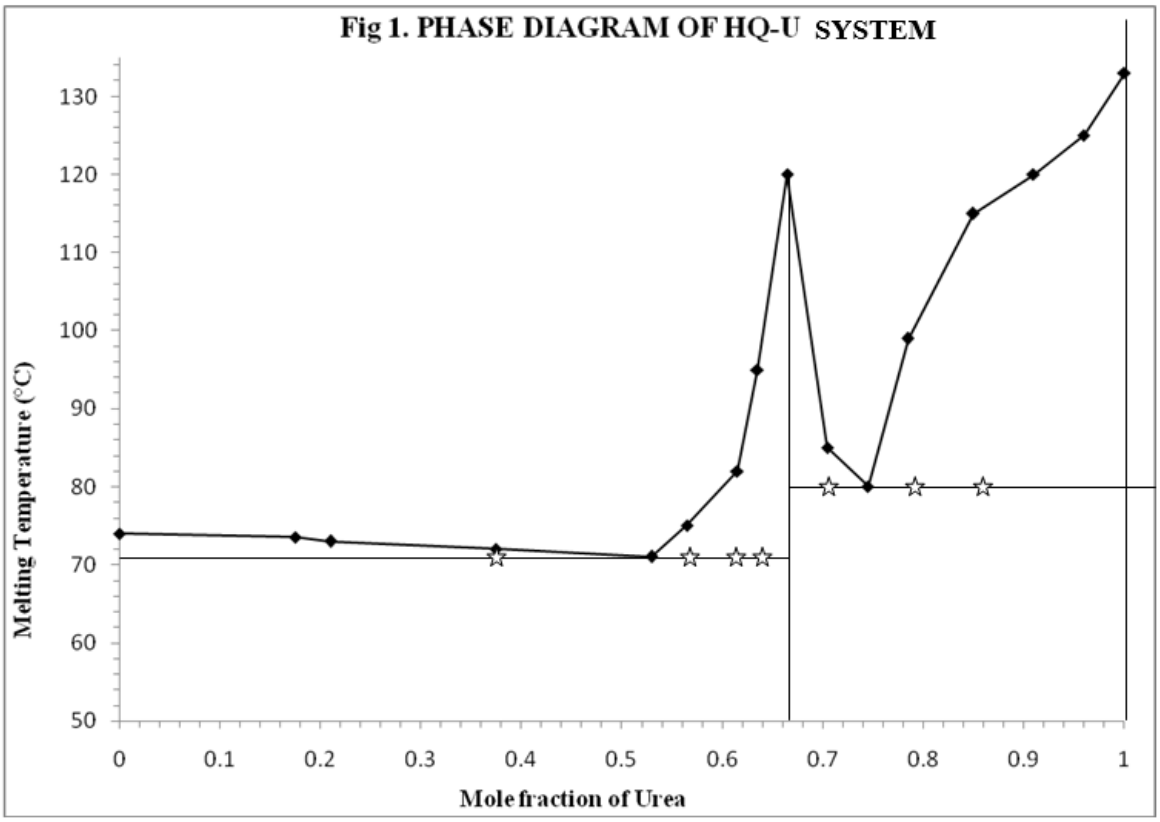

Table 1: Phase composition, melting temperature, values of entropy of fusion per unit volume (ΔS_v), heat of fusion(ΔH), interfacial energy(σ), grain boundary energy(σ_{gb}), Gibbs-Thomson coefficient (τ) and roughness parameter(α)

Alloy	χ_{HQ}	χ_U	MP	ΔH (J/mol)	ΔS (J/mol/K)	α	$\sigma(J/m^2) \times 10^2$	$\sigma_{gb}(J/m^2) \times 10^2$	ΔS_v $kJK^{-1}m^{-3}$	τ (Km) $\times 10^5$
A1	0.825	0.175	73.5	17860	51.54	6.20	2.810	5.429	417	1.30
A2	0.790	0.210	73	17692	51.13	6.15	2.835	5.476	425	1.29
A3	0.625	0.375	72	16900	48.99	5.89	2.972	5.741	468	1.23
E1	0.470	0.530	71	16156	46.97	5.65	3.143	6.071	522	1.16
A4	0.435	0.565	75	15988	45.94	5.53	3.189	6.160	530	1.16
A5	0.385	0.615	82	15748	44.36	5.34	3.261	6.300	541	1.16
A6	0.365	0.635	95	15652	42.53	5.12	3.292	6.360	531	1.20
C	0.335	0.665	120	15508	39.46	4.75	3.342	6.456	511	1.26
A7	0.295	0.705	85	15316	42.78	5.15	3.413	6.594	583	1.13
E2	0.255	0.745	80	15124	42.84	5.15	3.492	6.746	615	1.10
A8	0.215	0.785	99	14932	40.14	4.83	3.579	6.915	610	1.13
A9	0.150	0.850	115	14620	37.68	4.53	3.742	7.230	632	1.14
A10	0.090	0.910	120	14332	36.47	4.39	3.923	7.578	676	1.12
A11	0.040	0.960	125	14092	35.41	4.26	4.101	7.923	720	1.10
HQ			74	18700			2.705	5.226	317	1.65
UREA			133	13900			4.268	8.245	754	1.09

Table 2: Value of partial and integral excess Gibbs free energy (g^E), enthalpy (h^E) and entropy (s^E) of HQ – U system

Alloy	g_{HQ}^{-E} J/mol	g_U^{-E} J/mol	g^E J/mol	h_{HQ}^{-E} J/mol	h_U^{-E} J/mol	h^E J/mol	s_{HQ}^{-E} J/mol/K	s_U^{-E} J/mol/K	s^E J/mol/K
A1	527.24	2984.08	957.19	235386.65	1183937.06	401382.97	677.80	3408.23	1155.63
A2	624.20	2435.24	1004.52	149286.30	618048.46	247726.35	429.66	1779.23	713.07
A3	1240.34	724.92	1047.06	234630.91	408318.18	299763.63	676.49	1181.43	865.85
E1	1997.71	-306.90	776.27	113874.93	103666.44	108464.43	325.22	302.25	313.05
A4	2462.28	-333.86	882.46	-814.32	-129.61	-427.46	-9.42	0.59	-3.76
A5	3248.34	-311.25	1059.19	-9174.80	-7937.07	-8413.60	-34.99	-21.48	-26.68
A6	4215.29	88.45	1594.75	-14641.19	-11566.98	-12689.07	-51.24	-31.67	-38.81
A7	4226.34	-602.92	821.71	-11475.89	-10877.15	-11053.78	-43.86	-28.70	-33.17
E2	4333.78	-950.60	396.92	4515.67	-5953.70	-3284.01	0.52	-14.17	-10.43
A8	6101.27	-415.36	985.72	-2646.17	-9503.09	-8028.85	-23.51	-24.43	-24.23
A9	8329.30	-92.00	1171.20	30967.57	-5135.13	280.27	58.35	-13.00	-2.30
A10	10346.69	-136.92	806.60	138244.21	1621.95	13917.96	325.44	4.48	33.36
A11	13399.59	-138.81	402.72	209237.26	-4402.61	4142.98	492.05	-10.71	9.40

Table 3: Value of partial and integral mixing of Gibbs free energy (ΔG^M), enthalpy (ΔH^M) and entropy (ΔS^M) of HQ – U system

Alloy	ΔG_{HQ}^{-M} J/mol	ΔG_U^{-M} J/mol	ΔG^M J/mol	ΔH_{HQ}^{-M} J/mol	ΔH_U^{-M} J/mol	ΔH^M J/mol	ΔS_{HQ}^{-M} J/mol/K	ΔS_U^{-M} J/mol/K	ΔS^M J/mol/K
A1	1.60	14.49	-378.72	527.24	2984.08	957.19	1.60	14.49	3.86
A2	1.96	12.98	-473.95	624.20	2435.24	1004.52	1.96	12.98	4.27
A3	3.91	8.15	-850.52	1240.34	724.92	1047.06	3.91	8.15	5.50
E1	6.28	5.28	-1201.00	1997.71	-306.90	776.27	6.28	5.28	5.75
A4	6.92	4.75	-1098.49	2462.28	-333.86	882.46	6.92	4.75	5.69
A5	7.94	4.04	-907.84	3248.34	-311.25	1059.19	7.94	4.04	5.54
A6	8.38	3.78	-413.06	4215.29	88.45	1594.75	8.38	3.78	5.46
A7	10.15	2.91	-983.69	4226.34	-602.92	821.71	10.15	2.91	5.04
E2	11.36	2.45	-1269.37	4333.78	-950.60	396.92	11.36	2.45	4.72
A8	12.78	2.01	-624.11	6101.27	-415.36	985.72	12.78	2.01	4.33
A9	15.77	1.35	-192.39	8329.30	-92.00	1171.20	15.77	1.35	3.51
A10	20.02	0.78	-181.91	10346.69	-136.92	806.60	20.02	0.78	2.52
A11	26.76	0.34	-153.00	13399.59	-138.81	402.72	26.76	0.34	1.40

Table 4: Value of volume free energy change (ΔG_v) during solidification for HQ – U system of different undercoolings (ΔT)

Alloy	ΔG_v(J/cm^3)					
	1.0	1.5	2.0	2.5	3.0	3.5
A1	0.4165	0.6247	0.8329	1.0412	1.2494	1.4577
A2	0.4246	0.6368	0.8491	1.0614	1.2737	1.4859
A3	0.4676	0.7014	0.9351	1.1689	1.4027	1.6365
E1	0.5216	0.7824	1.0432	1.3040	1.5648	1.8256
A4	0.5298	0.7947	1.0596	1.3245	1.5894	1.8543
A5	0.5412	0.8118	1.0824	1.3530	1.6236	1.8942
A6	0.5312	0.7968	1.0624	1.3280	1.5936	1.8592
C	0.5110	0.7665	1.0220	1.2776	1.5331	1.7886
A7	0.5827	0.8741	1.1654	1.4568	1.7481	2.0395
E2	0.6154	0.9231	1.2308	1.5385	1.8462	2.1539
A8	0.6098	0.9148	1.2197	1.5246	1.8295	2.1345
A9	0.6317	0.9476	1.2635	1.5794	1.8952	2.2111
A10	0.6760	1.0140	1.3520	1.6900	2.0280	2.3660
A11	0.7197	1.0796	1.4394	1.7993	2.1591	2.5190
HQ	0.3167	0.4750	0.6334	0.7917	0.9501	1.1084
UREA	0.7542	1.1312	1.5083	1.8854	2.2625	2.6396

Table 5: Critical size of nucleus (r*) at different undercoolings (ΔT)

Alloy	r*(nm)					
	1.0	1.5	2.0	2.5	3.0	3.5
A1	135.0	89.97	67.48	53.98	44.98	38.56
A2	133.5	89.03	66.77	53.42	44.51	38.15
A3	127.1	84.74	63.55	50.84	42.37	36.32
E1	120.5	80.33	60.25	48.20	40.17	34.43
A4	120.4	80.25	60.19	48.15	40.13	34.39
A5	120.5	80.34	60.26	48.21	40.17	34.43
A6	124.0	82.64	61.98	49.58	41.32	35.42
C	130.8	87.19	65.39	52.32	43.60	37.37
A7	117.2	78.10	58.58	46.86	39.05	33.47
E2	113.5	75.66	56.74	45.40	37.83	32.43
A8	117.4	78.25	58.69	46.95	39.13	33.54
A9	118.5	78.98	59.24	47.39	39.49	33.85
A10	116.1	77.37	58.03	46.42	38.68	33.16
A11	114.0	75.98	56.99	45.59	37.99	32.56
HQ	170.8	113.9	85.42	68.34	56.95	48.81
UREA	113.2	75.46	56.59	45.28	37.73	32.34

Table 6: Talue of critical free energy of nucleation (ΔG*) for alloys of HQ – U system at different undercooling(ΔT)

Alloy	ΔG*(J)					
	1.0	1.5	2.0	2.5	3.0	3.5
A1	2.145E-15	9.531E-16	5.361E-16	3.431E-16	2.383E-16	1.751E-16
A2	2.118E-15	9.415E-16	5.296E-16	3.389E-16	2.354E-16	1.729E-16
A3	2.012E-15	8.941E-16	5.029E-16	3.219E-16	2.235E-16	1.642E-16
E1	1.912E-15	8.498E-16	4.780E-16	3.059E-16	2.125E-16	1.561E-16
A4	1.936E-15	8.606E-16	4.841E-16	3.098E-16	2.152E-16	1.581E-16
A5	1.985E-15	8.822E-16	4.962E-16	3.176E-16	2.205E-16	1.620E-16
A6	2.120E-15	9.422E-16	5.300E-16	3.392E-16	2.355E-16	1.731E-16
C	2.395E-15	1.065E-15	5.989E-16	3.833E-16	2.662E-16	1.955E-16
A7	1.963E-15	8.725E-16	4.908E-16	3.141E-16	2.181E-16	1.603E-16
E2	1.885E-15	8.377E-16	4.712E-16	3.016E-16	2.094E-16	1.539E-16
A8	2.067E-15	9.185E-16	5.166E-16	3.307E-16	2.296E-16	1.687E-16
A9	2.201E-15	9.783E-16	5.503E-16	3.522E-16	2.446E-16	1.797E-16
A10	2.214E-15	9.839E-16	5.535E-16	3.542E-16	2.460E-16	1.807E-16
A11	2.232E-15	9.922E-16	5.581E-16	3.572E-16	2.481E-16	1.822E-16
HQ	3.309E-15	1.470E-15	8.272E-16	5.294E-16	3.676E-16	2.701E-16
UREA	2.291E-15	1.018E-15	5.729E-16	3.666E-16	2.546E-16	1.871E-16